Materials Physics and Mechanics 47 (2021) 483-492 Received: May 19, 2021

SSRT METHOD: APPLICATION TO STUDYING THE MECHANISM OF STRESS CORROSION CRACKING IN STEELS AND ALLOYS (OVERVIEW)

A.A. Kharkov, A.A. Alkhimenko*, N.O. Shaposhnikov, E.L. Alekseeva

Peter the Great St.Petersburg Polytechnic University (SPbPU), Saint-Petersburg, Russian Federation

*e-mail: alkhimenko_aa@spbstu.ru

Abstract. The paper briefly describes the slow strain rate testing (SSRT) method used for steels and alloys, considering the stress and strain criteria for assessing the sensitivity of materials to stress corrosion cracking (SCC). We pointed out the clear benefits of the SSRT method over static SCC testing. We reviewed the modern theories of the main possible mechanisms of SCC, typically including alternating stages of anodic dissolution and hydrogen embrittlement during the initiation and propagation of cracks. The given examples indicate that electrochemical studies are necessary to understand the conditions when SCC might develop following one of two mechanisms. Furthermore, we substantiated metallographic analysis and investigations on the fracture surface of the samples to establish the cracking trajectories and the failure behavior. The brief overview presents examples of applying the SSRT method to testing low-alloy, stainless steels, aluminum, and nickel alloys in various corrosive environments.

Keywords: steels, stress corrosion cracking, SSRT method, metallography, fracture structure

1. Introduction

The first studies considering slow strain rate tests for stress corrosion cracking (SCC) appeared about half a century ago [1,2]. In contrast to traditional SCC tests at constant stress or constant strain rate [3-9], slow strain rate tests (SSRT) took less type for a material sensitive to the corrosive environment. While static tests lasted for 720–1000 hours [10,11], the time for the SSRT method ranged from several hours to 2-5 days [12]. Specimen failure during slow strain rate tests is either brittle due to corrosion cracking with partial or complete loss of ductility, or ductile, depending on the degree to which the material is sensitive to SCC in a given environment.

Even though the static loading and slow strain rate tests are seemingly different, the mechanism of crack propagation is the same. Crack propagation under a constant load also occurs at a slow rate of dynamic deformation (creep) originating at stress raisers. A structural defect or localized corrosion damage can act as such a raiser.

Because SSRT offers much shorter testing times compared to the static methods, and there is a good agreement between the data on the corrosion susceptibility of steels obtained by both methods [15], this method is preferable for studies on the SCC mechanism and for comparative tests of different materials.

SCC analysis often involves additional electrochemical studies, which consist of constructing the cathodic and anodic polarization curves in the same corrosive environment used for SCC tests of the material [16-19]. Metallographic methods analyzing the metal

http://dx.doi.org/10.18149/MPM.4732021_9

structure and the failure surface of the specimens fractured in the SCC tests are applied to understand the propagation behavior of corrosion cracks (intergranular or transgranular) [17-22].

The strain rate is an important choice in the SSRT method. What matters is that there should be enough time for electrochemical processes of metal dissolution and diffusion processes supplying oxidant to the crack tip to pass at a given deformation rate. The strain rates recommended by existing standards for testing steels and alloys are in the range of 10^{-7}-10^{-5} s^{-1}. Slow strain rate tests start at zero loads, continuing until specimen fracture; a tensile stress-strain curve is constructed. To detect the effect of the corrosive environment, a similar curve of the tested material is constructed for comparison in an inert environment.

One of the criteria characterizing the degree of corrosion susceptibility of material in SSRT is the relative strain at which specimen fracture starts in a corrosive environment (ε_{scc}). Another criterion is the stress at which crack propagation starts (σ_{scc}) [23,24]. The stress at which a crack initiates in a corrosive environment is determined from the point where the curves for the inert and the corrosive environment diverge. The ratios of ε_{scc} and σ_{scc} to the relative strain and the fracture stress, obtained during tests in the inert environment, can also be used. According to [25], the strain criterion, which depends on the environment, temperature, and material properties, can characterize its state under static, quasi-static, and cyclic loading. Compared to the stress criterion, it more adequately reflects the physical nature of the fracture associated with stress corrosion cracking and how it is influenced by external and internal factors; the stress criterion is convenient as a direct characteristic in time-to-failure calculations of products and structures.

If failure assessment diagrams are not plotted for the samples, the ratio of contraction/elongation at break of the specimens tested in the corrosive or inert environment (this is recommended by the NACE TM 0198 standard [26]), or the ratio of the time to fracture in the environment and the air [27] can be used as criteria.

The goal of this study is to review mechanisms of stress corrosion cracking and features of slow strain rate testing methods to access resistance to cracking for various materials.

2. Modern understanding of SCC mechanisms

Phelps proposed to use cathodic polarization to describe the SCC mechanism at the NACE Corrosion Conference in 1969. If SCC is suppressed during cathodic polarization, it can be assumed that cracking occurs following the mechanism of anodic dissolution (AD). Conversely, if cathode polarization accelerates, SCC is assumed to proceed via the mechanism of hydrogen embrittlement (HE). However, multiple subsequent studies have established that both the stage of electrochemical dissolution and the stage of hydrogen embrittlement occur in the overwhelming majority of cases provided there is no external polarization as the crack initiates and especially propagates.

The entire SCC process is divided into three stages: crack initiation, crack propagation under the influence of a corrosive environment, and mechanical failure as the acting stresses exceed the material strength (Fig. 1) [28,29].

It is generally believed that the main SCC mechanism for high-strength steels with a yield stress grades over 800 MPa in acidic electrolyte solutions or under cathodic polarization is hydrogen embrittlement, where corrosive electrochemical reactions facilitate the penetration of hydrogen into a metal. The hydrogen introduced into steel due to diffusive processes spreads inside the metal at a certain velocity as it passes through the interstices of the crystal lattice. Measurements of the diffusion coefficient and the amount of hydrogen absorbed by the steel indicate that more hydrogen is trapped in the steel than it follows from the diffusion coefficient [30,31]. Consequently, some of the hydrogens are located in 'traps' such as vacancies, dislocations, defects, stacking faults, grain boundaries, twins, non-metallic

inclusions, and submicropores. There are suggestions that hydrogen is grouped around dislocations in the form of Cotrell atmosphere and moves with it during plastic deformation. The exact manner in which hydrogen interacts with dislocation has little importance for the process of stress corrosion cracking. What matters is that dislocations are the most mobile defects, and their number (concentration) increases with increasing stresses and strains [32]. Moreover, because the deformation must be plastic, the local microstresses must exceed the yield strength of the steel. Based on these provisions, it is believed that when hydrogen accumulates near mobile dislocations, local plastic flow initiates at the crack tip, with subsequent crack jumping due to hydrogen embrittlement [2,3,33-35]. SCC of high-strength steels follows the same mechanism under cathodic polarization. Figure 2 schematically shows the process of hydrogen-assisted stress corrosion cracking for low-alloy steel [11].

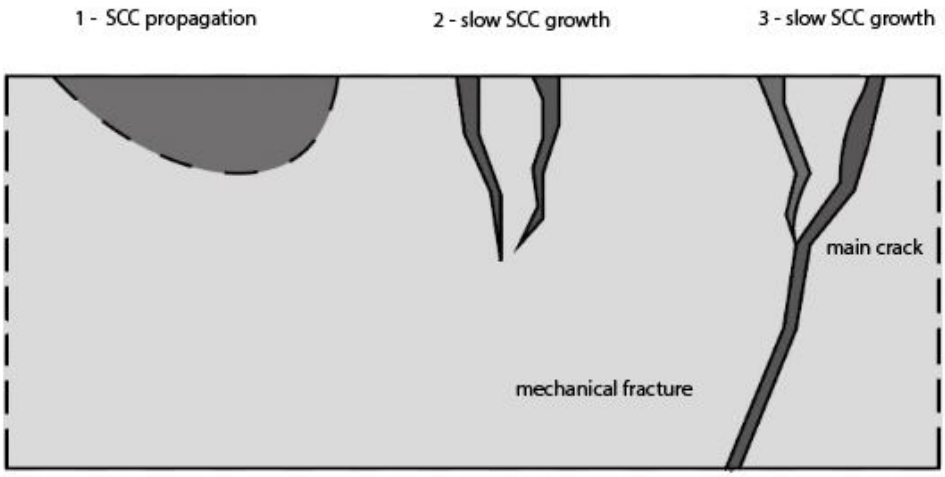

Fig. 1. Schematic crack propagation (1, 2, 3 correspond to the stages of fracture during SCC). According to the description from Ref. [29]

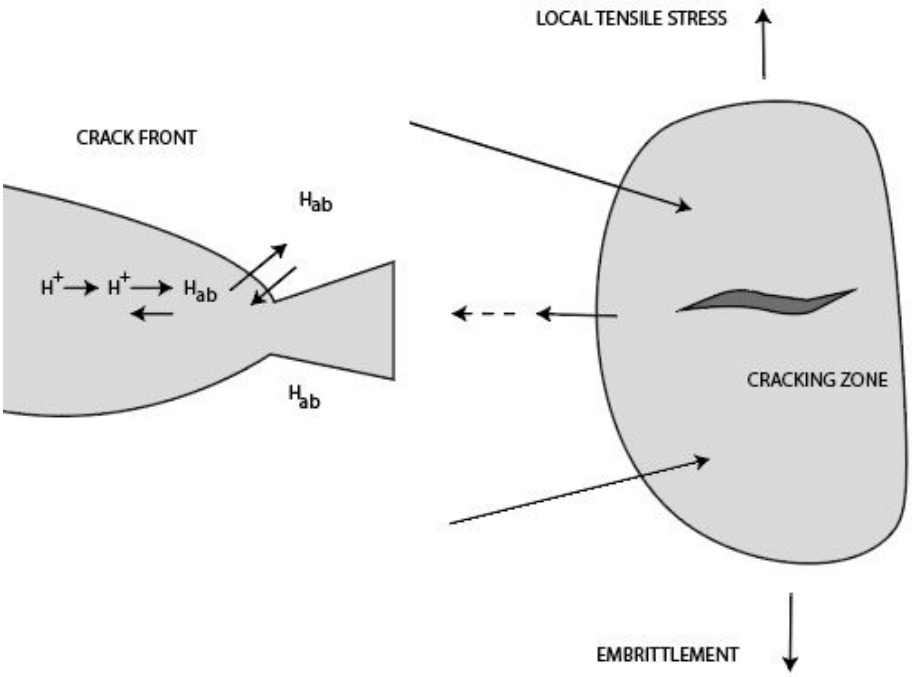

Fig. 2. Model of SCC following the hydrogen embrittlement mechanism (transport process: 1) ion transport, 2) electrochemical reaction, 3) absorption (hydrogen penetration), 4) diffusion. According to the description from Ref. [11]

The mechanism of anodic dissolution assumes that the local dissolution of the metal is accelerated at the crack tip. This is likely explained by a decrease in the electrochemical potential of the metal as it is deformed under stress concentration and destruction of the protective film, with a freshly formed surface opening as a result.

It is the general consensus that SCC of carbon and low-alloy steels occurs in neutral environments as a synergistic effect of mechanical stresses, anodic dissolution, and absorption of hydrogen by steel [8,9,11,35-43].

In view of the above, the mechanism of the SCC of low- and medium-alloy steels can be represented as follows. Uneven corrosion points start to form on the surface of steel due to microinhomogeneities on the surface, acting as small stress raisers. Microcracks near the surface opened as a result of corrosion, can also serve as such raisers. Hydrogen ions from the solution are adsorbed on the surface of the metal and capture its electrons to be converted back into atoms. Next, atomic hydrogen penetrates into the steel and concentrates at the tips of corrosive or other defects, which serve as stress raisers. If the level of local stresses at the tip of some defect exceeds the yield point of the steel, a very slow plastic flow initiates. This process further contributes to increasing the hydrogen concentration; as a certain critical deformation is reached due to hydrogen embrittlement, the crack jumps to a distance at which the critical deformation value is exceeded. As a result, the metal surface at the top of the propagating crack and its opening edges at this moment is absolutely clean (fresh) from any corrosion products, rendering it highly corrosive [11].

Thus, the crack grows in sequential stages. The stage when hydrogen accumulates and approaches the tip is succeeded by the stage when plastic deformation accumulates and a crack jump occurs. Notably, both stages are always accompanied by electrochemical dissolution of the metal at the tip of the growing crack. An exception to this is SCC at high cathodic polarization when the process of metal dissolution becomes thermodynamically impossible. It follows from here that the growth of a corrosion crack is a quasi-brittle process since the crack propagates abruptly.

Different scenarios can unfold depending on the aggressiveness of the corrosive environment. Given an acidic environment with a high concentration of hydrogen ions, the metal at the crack tip dissolves at the same time as atomic hydrogen penetrates into the steel. Hydrogen first accumulates near mobile dislocations, local plastic flow initiates at the crack tip, and subsequent crack jumping occurs due to hydrogen embrittlement [2,3,34,35,44]. SCC of high-strength steels follows the same mechanism under cathodic polarization [17,19,27].

Hydrolysis of corrosion products, i.e., the ions introduced into the solution during the dissolution of metal inside the crack, contributes to the accumulation of hydrogen ions. For example, 3 hydrogen ions are produced with the hydrolysis of one chromium ion. This means that the solution inside the growing crack is constantly acidified.

In the case of transgranular crack propagation in a neutral corrosive environment with a low concentration of hydrogen ions, the stage of surface dissolution at the crack tip may prevail over the stage of hydrogen embrittlement, which should lead to blunting of the crack tip. This weakens the effect of the crack as a stress raiser on the microplastic flow intensity and can completely stop the crack's further growth.

In the case of intergranular corrosion cracking [9,16,33,34], the crack propagates deep into the metal at the stage of anodic dissolution, along with the most active spots, which are typically grain boundaries. The most common locations for cracks to initiate in austenitic corrosion-resistant steels, aluminum and high-nickel alloys, whose surface is covered with a passive protective film, are pitting areas, evolving, for example, upon exposure to chlorides in the solution. Next, crack growth can also occur by alternating stages of electrochemical dissolution of the crack tip, accumulation of hydrogen atoms in the metal at the tip, the onset of plastic flow until critical deformation is reached, and brittle jumps by the distance of the

zone that underwent embrittlement. The most favorable path of crack propagation for such steels and alloys is along the grain boundaries, where chromium carbides and intermetallic compounds are precipitated. As a result, the regions adjacent to the grains are depleted by chromium, with certain stress micro-concentration produced [22,45-48].

3. The SSRT method in studies of the SCC mechanism of steels and alloys in various corrosive environments

Extensive experience has been accumulated for using the SSRT method in SCC testing for various corrosive environments of low-alloy and stainless steels, aluminum, and nickel alloys, as well as their welded joints. Applications of these structural materials cover major industries such as oil and gas, including hydrocarbon transportation and processing, energy, including nuclear, aviation, shipbuilding, and others. For this reason, the environments used for the test can considerably differ.

Many recent studies consider the SCC processes in low-alloy steels and welded joints are used in gas transmission pipelines. Since electrochemical methods are used to protect the outer surfaces of gas pipelines against corrosion from wet soil, SCC testing of pipe steels is carried out under cathodic polarization.

Reference [16] considered the cracking behavior of X52 pipe steel in a bicarbonate-carbonate solution containing chlorides and sulfates (NS4 solution [40]) at pH 6.5 and pH 9.5 with the applied potentials ranging from -785 mV to -2000 mV during the SSRT procedure with the specimen strain rate of 1.31×10^{-5} s^{-1}. The specimens had a working area with a diameter of 3.81 mm and a length of 25.4 mm. To understand whether the crack propagation was controlled by hydrogen embrittlement or anodic dissolution, polarization curves were measured at a potential sweep rate of 0.5 mV/s and 50 mV/s, simulating the electrochemical conditions on the walls and at the crack tip, respectively [17,49]. Metallographic studies were carried out after the tests.

In [16] the tensile stress-strain curves for the X52 steel obtained in NS4 solution at pH 6.5 and pH 9.5 with different levels of cathodic polarization specimen fracture occurs at potentials of -785 mV and -950 mV when deformation is close to or slightly higher than in air. This means that steel does not exhibit a tendency to SCC. This is confirmed by the viscous nature of specimen fracture. As the potential shifts further to the cathode region, the sensitivity to SCC increases. It is believed that the electrochemical conditions at the crack tip can be more accurately described with a polarization curve measured under fast potential scanning, while slow potential scanning better suits the conditions on the walls of a propagating crack [17]. Anodic processes of metal dissolution at the tip and on the walls of the crack are impossible at potentials below -950 mV; therefore, SCC can only happen by the mechanism of hydrogen embrittlement. The walls of the crack are cathodically polarized in the potential range from -780 mV to -950 mV, and its tip is anodically polarized. Consequently, SCC may be controlled by anodic dissipation in this potential range. The anodic dissolution mechanism becomes predominant at higher positive potentials. Similar conclusions were obtained during SCC tests by the SSRT method in a neutral solution with various applied potentials at a strain rate of 5×10^{-7} s^{-1} for the X70 pipe steel [17] and under static conditions at a stress of 95% yield strength for the X80 and X100 steels [50].

It was established by SSRT that ferritic/pearlitic steels of the AISI4140 and AISI4340 types have an increased tendency to SCC with an increase in the nickel content from 0.26% to 3% under cathodic polarization in the potential range of -1.05-2V (silver chloride electrode) [51]. The results obtained are in line with the recommendations of the ISO 15156:2 standard limiting the nickel content (to no higher than 1%) in low-alloy pipe steels for petroleum and gas environments containing hydrogen sulfide.

The SSRT method has been successfully used to test welded joints made of steel and alloys. Reference [52] considered the influence of ultrasonic nanocrystal surface modification in welded joints of ASTM A109 steel in weakly mineralized water at 60°C. Metallographic studies revealed a decreased tendency to SCC after ultrasonic treatment because the Widmanstaetten structure transformed into polygonal ferrite with a refined microstructure.

Tests of the welded joints of the X100 steel in bicarbonate-carbonate solution at 75°C (pH 9.5) at a strain rate of 2×10^{-6} s^{-1} revealed that the steel was sensitive to SCC. Metallographic studies and analysis of the fracture surfaces of the specimens revealed that cracking was intergranular at a given pH, and transgranular under cathodic polarization (potential below -890 mV) [53]. Reference [54] reports on the tests of welded joints for the E690 bainitic steel in a simulated marine atmosphere containing SO_2. The results indicate that the metal in the heat-affected zone had a high sensitivity to SCC. SCC tests were conducted for flat-plate specimens with the longitudinal direction perpendicular to welded joint and fusion line at the center at a strain rate of $0.5\times10^{-6}s^{-1}$. The specimens were sprayed with a solution containing 3.5% NaCl + 0.01 mol/L $NaHSO_3$ with pH of approximately 3.8 at approximately 25°C.

The SCC tendency in stainless steels, often used as pipes and tube sheets of heat exchangers at power plants, are carried out in water solutions at temperatures above 100°C. Slow strain rate testing of the 310S steel was performed after various heat treatments (austenitization, with annealing at 1050°C for 1 hour followed by water-quenching; sensitization for 100 hours at 650°C followed by air-cooling). The tests were carried out at a strain rate of 1×10^{-6} s^{-1} in a 3.75 M NaOH + 0.64 M Na_2S solution at 170°C, and for comparison in dry sand heated to the same temperature. It was found that the steel sensitized at 650° C exhibited a strong tendency to intergranular SCC.

Metallographic studies revealed that cracking was intergranular. The reason for this is Cr-depleted zones form along grain boundaries in the zones where Cr-rich $M_{23}C_6$ precipitates are formed. Tests of the 347N stainless steel at a strain rate of $1\times10^{-6}s^{-1}$ in supercritical water of supercritical parameters at 550, 600 and 650° C and dissolved oxygen content of 2 ppb and < 10 ppb, with subsequent metallographic studies, indicate that cracking bears an intergranular character for all of the given parameters [46]. Similar results were obtained for the Type 347, serving as heater tube in a petroleum refinery as heater tube at 620°C for 31 years, after testing by the SSRT method in a NaCl+Na2S2O3 solution [45]. Chromium carbide colonies were discovered along the grain boundaries of the steel, producing intergranular fracture during the SCC tests.

Reference [20] investigated the effect of nitrogen and carbon on the SCC susceptibility of Fe-Cr-Mn-based stainless steel in a sodium chloride solution. The tests were carried out at a strain rate of $1\times10^{-6}s^{-1}$ in a 0.6 M NaCl solution at 25°C and in a 2 M NaCl solution at 50°C at a constant anodic applied potential of +50mV versus corrosion potential. Electrochemical and metallographic studies established that additional alloying of steel with nitrogen and carbon increases its resistance to SCC by increasing the pitting corrosion resistance and the repassivation tendency (i.e., pitting extinction).

A Ni-based superalloy 718 (UNS-N07718) was tested for SCC by SSRT at strain rates of 5×10^{-5} s^{-1} in hydrogen gas at 0.7, 12, and 95 MPa [21]. Apparently, cracking becomes more pronounced with increasing hydrogen pressure. While ductile pitted structures can be observed in a considerable part of the fracture surface, zones characteristic for brittle failure are also were presented. The authors propose a mechanism describing the crack initiation and propagation upon exposure of a Ni-based alloy 718 to gaseous hydrogen sulfide, schematically shown in Fig. 3.

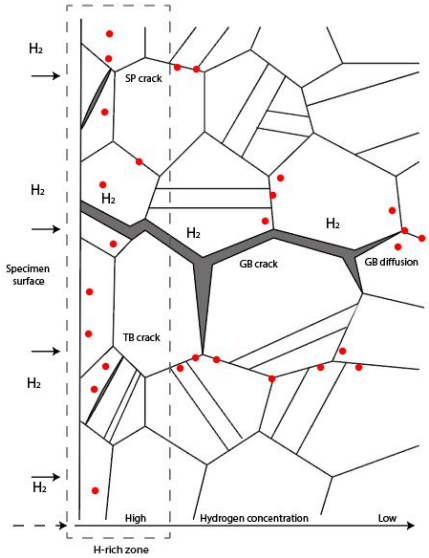

Fig. 3. Schematic initiation and propagation of cracks during hydrogen-induced SCC of Ni-based alloy 718 (SP are cracks propagating along slip planes; TB cracks propagating along twin boundaries; GB cracks propagating along grain boundaries). According to the description from Ref. [21]

Cracks are formed due to the interaction of atomic hydrogen, penetrating into the alloy by diffusion, with dislocations concentrated on slip planes and their boundaries (transgranular cracking). Next, upon reaching the grain boundaries, hydrogen can propagate along with them, causing the intergranular fracture.

The SCC tendency of a friction stir welded joint of a high-strength Al-Zn-Mg alloy was studied by SSRT according to the specification of GB 15970.7–2000 [55] at a strain rate of 1×10^{-6} s^{-1} in 3.5% NaCl solution [22]. It was found that inclusions containing Fe, Si, and Mn, as well as intermetallic Al3ScxZr1-x compounds, act as stress raisers, contributing to cracking. Local anodic dissolution around such microparticles leads to the initiation of cracks. In this case, cracking occurs by alternating mechanisms of anodic dissolution and hydrogen embrittlement.

4. Conclusions

1. The advantage of the SSRT method over the methods of static SCC tests is shown, and the concepts of deformation criteria for assessing the sensitivity of materials to stress corrosion cracking during testing by the SSRT method are given.
2. The generally accepted basic concepts of the mechanism of SCC of steels and alloys, according to which the nucleation and cracks growth is carried out by sequential alternation of the stages of anodic dissolution and hydrogen embrittlement in the process of local plastic deformation of a metal at the tip of a growing crack.
3. Examples of the application of the SSRT method are given when carrying out tests for SCC in various corrosive environments of low-alloy and stainless steels, alloys on an aluminum and nickel base, as well as their welded joints.
4. An important role in the study of the SCC mechanism of the use of electrochemical research is shown, consisting in the construction of the cathodic and anodic polarization curves in the same corrosive environment, which is used in testing the material for RS, as well as metallographic methods for analyzing the structure and surface of the fracture destroyed during testing by the SSRT method samples, to reveal the nature of the propagation of a corrosion crack (intergranular or transcrystalline).

Acknowledgments. *The research is partially funded by the Ministry of Science and Higher Education of the Russian Federation as part of World-class Research Center program: Advanced Digital Technologies (contract No. 075-15-2020-934 dated 17.11.2020)*

References

[1] Parkins RN, Mazza F, Royella JJ, Skully JK. Corrosion testing methods for stress corrosion cracking resistance. *Metal protection*. 1973;9(5): 515-540. (In Russian)
[2] Scully JR, Moran PJ. Influence of Strain on the Environmental Hydrogen-Assisted Cracking of a High Strength Steel in Sodium Chloride Solution. *Corrosion.* 1988;44(3): 176-185.
[3] Azhogin FF. *Stress corrosion cracking and protection of high strength steels.* Moscow: Metallurgy; 1974. (In Russian)
[4] Brown BF. *Stress Corrosion Cracking in High Strength Steels and in Aluminium and Titanium Alloys*. Washington: NRL; 1972
[5] Vasilenko II, Melekhov RK. *Stress corrosion cracking of steels*. Kiev: Naukova dumka; 1977. (In Russian)
[6] Fomin GS. *Corrosion and corrosion protection.* Moscow: Publishing House of Standards; 1994. (In Russian)
[7] Oryshchenko AS, Mushnikova SY, Kharkov AA, Kalinin GY. Study of stress corrosion cracking of austenitic steels in seawater. In: *Proc. The European Corrosion Congress EUROCORR'2010.* 2010.
[8] Schreier LL. *Corrosion.* London: Elsivier; 1976.
[9] Ryabchenkov AV, Nikiforova VM. *Intergranular corrosion and corrosion of metals in a stressed state. The role of electrochemical factors in the process of stress corrosion cracking of austenitic steels.* Moscow: Metallurgy; 1969. (In Russian)
[10] *TM0177-2016-SG, Laboratory Testing of Metals for Resistance to Sulfide Stress Cracking and Stress Corrosion Cracking in H2S Environments*. Houston: NACE International; 2016.
[11] Konakova MA, Teplinskii YA. *Stress corrosion cracking of pipe steels*. St. Petersburg: Info-yes; 2004. (In Russian)
[12] Alkhimenko AA, Kharkov AA, Shemyakinskii BA, Shaposhnikov NO. Development of a methodology for accelerated testing of oil country tubular steels for stress corrosion cracking. *Factory laboratory. Diagnostics of materials.* 2020;86(9): 70-76. (In Russian)
[13] Kushnarenko VM. The question of corrosion cracking of metals under a constant load and slow tension, *Soviet Materials Science.* 1991;26: 530-533.
[14] Kadyrbekov VM, Kolesnikov VA, Pecherskii VA. Evaluation of the resistance of steels to stress corrosion cracking when tested at a constant strain rate. *Physical and Chemical Mechanics of Materials*. 1989;25(1): 39-42.
[15] Hoey GR, Revie RW, Ramsingh RR. Comparison of the slow strain rate technique and the NACE TM01-77 tensile test for determining sulfide stress cracking resistance. *Mater. Perfom*. 1987;26(10): 42-45.
[16] Javidi M, Bahalaou HS. Investigating the mechanism of stress corrosion cracking in near-neutral and high pH environments for API 5L X52 steel. *Corrosion Science*. 2014;80: 213-220.
[17] Liu ZY, Li XG, Cheng YF, Mechanistic aspect of near-neutral pH stress corrosion cracking of pipelines under cathodic polarization. *Corros. Sci.* 2012;55: 54-60.
[18] Marshakov AI, Ignatenko VE, Bogdanov RI, Arabey AB. Effect of electrolyte composition on crack growth rate in pipeline steel. *Corrosion Science*. 2014;83: 209-216.
[19] Zhang L, Li X, Du C, Huang Y. Effect of applied potentials on stress corrosion cracking of X70 pipeline steel in alkali solution. *Mater. Des*. 2009;30: 2259-2263.
[20] Ogawa Y, Takakuwa O, Okazaki S, Okita K, Funakoshi Y, Matsunaga H, Matsuoka S. Pronounced transition of crack initiation and propagation modes in the hydrogen-related

failure of a Ni-based superalloy 718 under internal and external hydrogen conditions. *Corrosion Sci.* 2019;161: 108-186.
[21] Deng Y, Peng B, Xu G, Pan Q, Ye R, Wang Y, Lu L,. Yin Z. Stress corrosion cracking of a high-strength friction-stir-welded joint of an Al-Zn-Mg-Zr alloy containing 0.25 wt% Sc, *Corrosion Science*. 2015;100: 57-72.
[22] Kharkov AA, Nemchikova LG, Mihnevich AP, Bilina SYu. Assessment of the tendency of steels to stress corrosion cracking when tested with a slow rate of deformation. *Technology of Shipbuilding*. 1990;3: 10-13. (In Russian)
[22] Mushnikova SY, Kharkov AA, Popov VI, Kalinin GY. Determination of the tendency to stress corrosion cracking of shipbuilding steels. Proceedings of international conference "Fundamental Aspects of Corrosion Materials Science and Metal Corrosion Protection", Moscow, 18-20 May 2011. (In Russian)
[23] Steklov OI, Polyarus AN. Resistance of materials to stress corrosion cracking. *Zashita Metallov*. 1990;16(5): 514-652. (In Russian)
[24] NACE Standard TM 0198-2011. *Slow Strain Rate Test Method for Screening Corrosion-Resistant Alloys for Stress Corrosion Cracking in Sour Oilfield Service*. Houston: NACE International; 2011.
[25] Volgina NI, Sharipnyazova JH, Khlamkova SS. *Method for Evaluating Stress Corrosion Cracking Resistance of Low Alloy Pipe Steels*. Patent RU 2 611699 C1. 2017.
[26] Gareev AG, Ivanov IA, Abdullin IG. *Prediction of corrosion-mechanical destruction of main pipelines*. Moscow: IRC Gazprom; 1997. (In Russian)
[27] Chuckalov MV. *Theory and practice of combating stress corrosion cracking on main gas pipelines.* Moscow: Makspress; 2016. (In Russian)
[28] Ignatenko VE, Marshakov AI, Marichev VA, Mikhailovskii YN, Petrov NA. Influence of cathodic polarization on the rate of stress corrosion cracking of pipe steels. *Protection of Metals.* 2000;36: 111-117.
[29] Liu Q, Atrens A. Reversible hydrogen trapping in a 3,5NiCrMoV medium strength steel. *Corrosion Science.* 2015;96: 112-120.
[30] Gareeva OA, Khudyakov MA, Klimov PV, Khajiev AD. Modeling of stress corrosion cracking of main pipelines. *Zashita metallov.* 2010;1(79): 87-92. (In Russian)
[31] Wang S, Martin ML, Sofronis P, Ohnuki S, Hashimoto N, Robertson IM. Hydrogen-induced intergranular failure of iron. *Acta Mater*. 2014;69: 275-282.
[32] Novak P, Yuan R, Somerday BP, Sofronis P, Ritchie RO. A statistical, physical based, micro-mechanical model of hydrogen-induced intergranular fracture in steel. *J. Mech. Phys. Solids.* 2010;58: 206-226.
[33] Marichev VA. Modern concepts of hydrogen embrittlement during delayed fracture. *Zashita metallov*. 1980;16(5): 531-543. (In Russian)
[34] Antonov VG, Baldin AV, Galliulin ZT et al. *Investigation of the conditions and causes of corrosion cracking of pipes of main gas pipelines.* Moscow: VNIIEgazprom; 1991. (In Russian)
[35] Arafin MA, Szpunar JA. A new understanding of intergranular stress corrosion cracking resistance of pipeline steel through grain boundary character and crystallographic texture studies. *Corros. Sci*. 2009;51: 119-128.
[36] Song FM. Predicting the mechanisms and crack growth rates of pipelines undergoing SCC at high pH. *Corros. Sci.* 2009;51: 2653-2657.
[37] Been J, King F, Sutherby RL. Environmentally assisted cracking of pipeline steels in near-neutral pH environments. In: *Proceedings of the Second International Conference on Environment-Induced Cracking of Metals.* 2004. p.221.
[38] Ignatenko VE, Kuznetsov YI, Arabey AB, Igoshin RV, Bogdanov RI, Marshakov AI. Application of SSRT to estimate the effect of corrosive medium on the liability of X70 pipe steel to stress corrosion cracking. *Int. J. Corros. Scale Inhib*. 2013;2(4): 318-336.
[39] Parkins RN, Blanchard WK, Detanty BS. Transgranular stress corrosion cracking of high pressure pipelines in contact with solutions of near-neutral pH. *Corrosion*. 1994;50: 394-408.

[40] Bulloch JH. Same effect of yield strength on the stress corrosion cracking behaviour of low alloy steels in aqueous environments at ambient temperatures. *Eng. Fail. Anal*. 2004;11: 843-856.
[41] Gu B, Luo J, Mao X, Hydrogen-facilitated anodic dissolution-type stress corrosion cracking of pipeline steels in near-neutral pH solution. *Corrosion.* 1999;55: 96-106.
[42] Kobayashi K, Omura T, Ueda M, Nakamura K. Effect of Testing Temperature on SSC Properties of Low Alloy Steel. In: *Proceedings of Corrosion*. 2006. p.06127.
[43] Ravindranath K, Tanoli N, Al-Wakaa D. Effect of Long-Term Service Exposure on the Localized Corrosion and Stress Corrosion Cracking Susceptibility of Type 347 Stainless Steel. *Corrosion*. 2018;74(3): 350-361.
[44] Guo X, Gao W, Chen K, Shen Z, Zhang L. Corrosion and Stress Corrosion Cracking Susceptibility of Type 347H Stainless Steel in Supercritical Water. *Corrosion*. 2018;74(1): 83-95.
[45] Jiao Y, Mahmood J, Zheng W, Singh PM, Kish JR. Effect of Thermal Aging on the Intergranular Stress Corrosion Cracking Susceptibility of Type 310S Stainless Steel Corrosion. *Corrosion*. 2018;74(4): 430-443.
[46] Ogawa Y, Takakuwa O, Okazaki S, Okita K, Funakoshi Y, Matsunaga H, Matsuoka S. Pronounced transition of crack initiation and propagation modes in the hydrogen-related failure of a Ni-based superalloy 718 under internal and external hydrogen conditions. *Corrosion Science*. 2019;161: 108186.
[47] Liu ZY, Li XG, Cheng YF. Mechanistic aspect of near-neutral pH stress corrosion cracking of pipelines under cathodic polarization. *Corros. Sci.* 2012;55: 54-60.
[48] Yan L, Gravel J, Kang J, Xu L, Arafin M. Occurrence of Near-Neutral pH Stress Corrosion Cracking in X80 and X100 Pipe Steels Under Various Cathodic Protection Conditions. *Corrosion.* 2018;74(9): 1033-1043.
[49] Husby H, Wagstaff P, Januzzi M, Johnsen R, Kappes M. Effect of nickel on the hydrogen stress cracking resistance of ferritic/pearlitic low alloy steels. *Corrosion.* 2018;74(70): 801-818.
[50] Kim Y, Kim W, Kim J. Influence of Ultrasonic Nanocrystal Surface Modification on the Corrosion and Stress Corrosion Cracking Behavior of Low Carbon Steel (ASTM A139) Welded Joint in the Simulated District Heating Environment. *Corrosion.* 2018;74(1): 112-122.
[51] Mustapha A, Charles EA, Hardie D. Evaluation of environment-assisted cracking susceptibility of a grade X100 pipeline steel. *Corrosion Science*. 2012;54: 5-9.
[52] Ma HC, Liu ZY, Du CW, HR Wang, Li XG, Zhang DW, Cui ZY. Stress corrosion cracking of E690 steel as a welded joint in a simulated marine atmosphere containing sulphur dioxide. *Corrosion Science*. 2015;100: 1-15.
[53] GB 15970.7-2000. National standard of China. *Corrosion of metals and alloys – stress corrosion testing – slow strain rate testing*.